Electronic Supplementary Material (ESI) for Lab on a Chip.

Supporting Information for

Controlled single-cell deposition and patterning by highly flexible hollow cantilevers

Vincent Martinez, ‡[a] Csaba Forró, [a] Serge Weydert, [a] Mathias J. Aebersold, [a] Harald Dermutz, [a]

Orane Guillaume-Gentil, [b] Tomaso Zambelli, [a] János Vörös, [a] and László Demkó[a]*

[a] Laboratory of Biosensors and Bioelectronics, Institute for Biomedical Engineering, ETH Zurich, CH-8092 Zurich, Switzerland.

[b] Institute of Microbiology, ETH Zurich, CH-8093 Zurich, Switzerland.

* corresponding author, demko@biomed.ee.ethz.ch

‡ martinez@biomed.ee.ethz.ch

This PDF file includes:

- Table S1
- Figures S1 – S7

	Precision		Complexity	Substrate	Throughput	Commercial availability
	number of cells	lateral				
Polymer cantilever	1-3 cells	~5µm	medium	any	~0.1 cells/sec	no
Micropipette[17,18]	1 (~80% success)	25-50 µm	low	wells	2-4 cells/sec	yes
Hollow AFM cantilever[19,20]	1	~10µm	medium	wells	not shown	yes
Laser-guided direct writing[21-23] (with/without guidance through optical fibers)	1	~1µm	medium	any	0.01 – 0.1 cells/sec	no
Optical tweezer[24,25]	1	not shown	medium	any	~0.02 cells/sec	yes
Micro-gripper,[26,27] dielectrophoresis tweezers,[28,29] and micro-magnets[30]	1	not shown	medium-high	any	not shown	no
Laser writing of cell donor layers[31-36] (LIF, AFA-LIFT, BioLP, MAPLE DW)	1-10 cells	20-500µm	medium	coated or dry substrate, large flat area	100 spots/sec	yes
Micro-valve[37-40]	1-5 cells	~500µm	low	mostly wells	up to 1000 drops/sec	yes
Modified inkjet (thermal and piezoelectric)[41-43]	1 (~85% success)	50-100 µm spot size	low	coated or dry substrate, large flat area	1000 spots/sec	yes
Modified inkjet (with camera control)[44,45]	1	40-50µm	medium	coated or dry substrate, large flat area	0.1 cells/sec	yes
Acoustic field[46,47]	0-10+ cells	80-400µm	high	dry substrate[29] or in liquid[30,31]	up to 10.000 spots/sec	no
Electrohydrodynamic[48-50]	0-10+ cells	~50-1000µm	medium	dry substrate	up to 100 drops/sec	yes

Table S1 Comparing the characteristics of the state-of-the-art technologies targeting additive single-cell patterning, based on and estimated by the indicated references. The first row corresponds to the technology developed and presented within this manuscript.

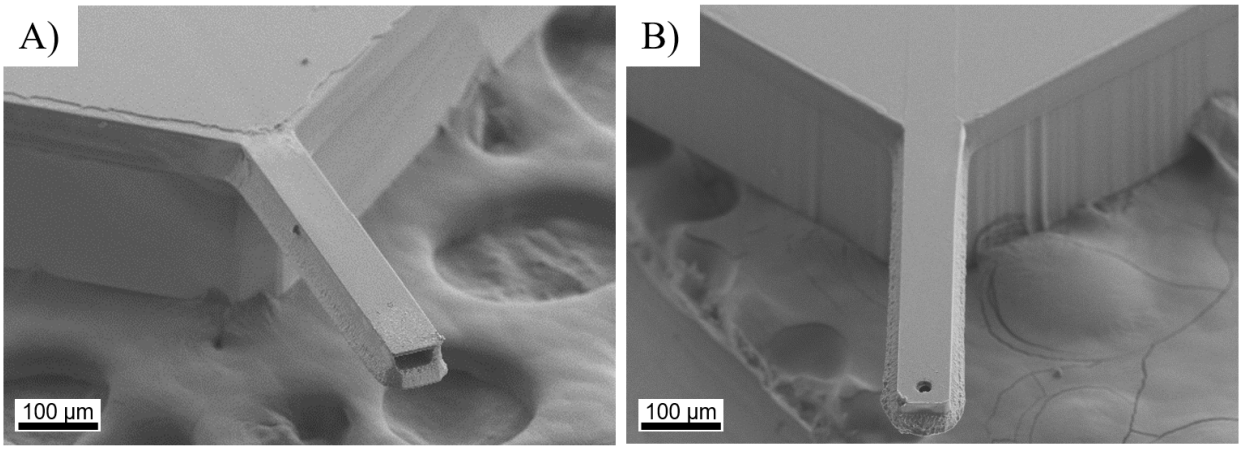

Fig. S1 Upside down SEM images of the different types of SU-8 cantilevers used for the different approaches. A) A micropipette-like design for experiments of configuration 1, with the aperture defined in the front plane of the cantilever identical in size to that of the microfluidic channel, 22 µm high and 50 µm wide. B) A cantilever with the aperture designed at the bottom plane for experiments of configurations 2 to 5. Aperture diameters of the fabricated cantilevers were ranging from 20 to 35 µm.

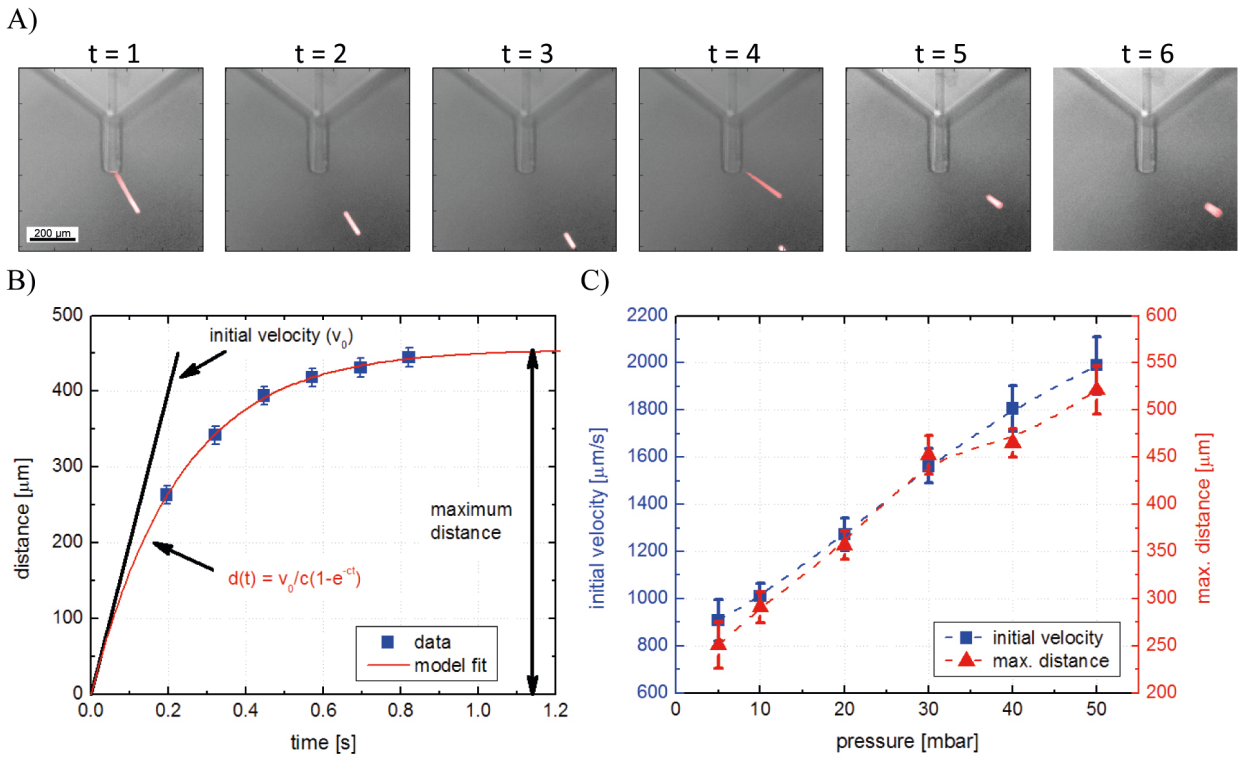

Fig. S2 Cell tracking of fluorescently labeled individual cells as a function of external pressure applied in the micropipette-like configuration. A) Individual frames recorded with a frequency of 8 frames per second were analyzed to identify the trajectories of the cells (shown in red). The length of the cantilever used here was 250 µm. B) A representative time–distance profile fitted with a flow model based on Stoke's (linear) drag. Lateral distances were measured from the cantilever aperture. C) Cell velocity at the aperture of the cantilever and the corresponding maximum distances cells can travel in the medium limited by the drag force. Results are presented as mean ± standard error after analyzing 203 individual trajectories, while dashed curves serve as visual guides only.

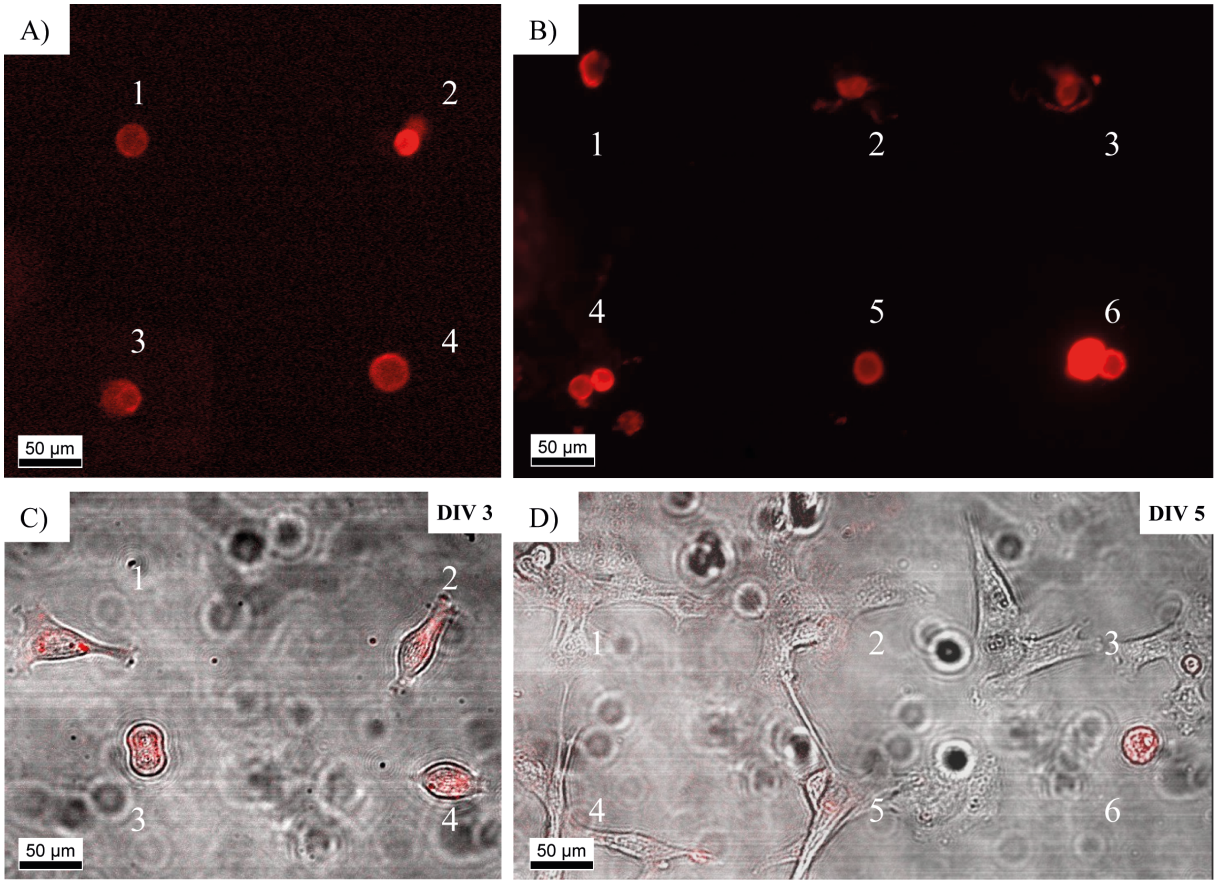

Fig. S3 Viability of fluorescently labeled myoblast cells after single-cell additive patterning (configuration 3) tracked for 2 different patterns. A) Fluorescence microscopy images of a grid with 4 and B) a grid with 9 cells (at 6 different deposition locations) right after deposition. C) Merged fluorescent and bright field images of the pattern A) after 3 DIV, while D) corresponds to pattern B) after 5 DIV. Most of the cells stayed healthy after deposition, indicated by their spreading and proliferation. Poor image quality in the bright field mode were due to objective contamination during the course of this experiment.

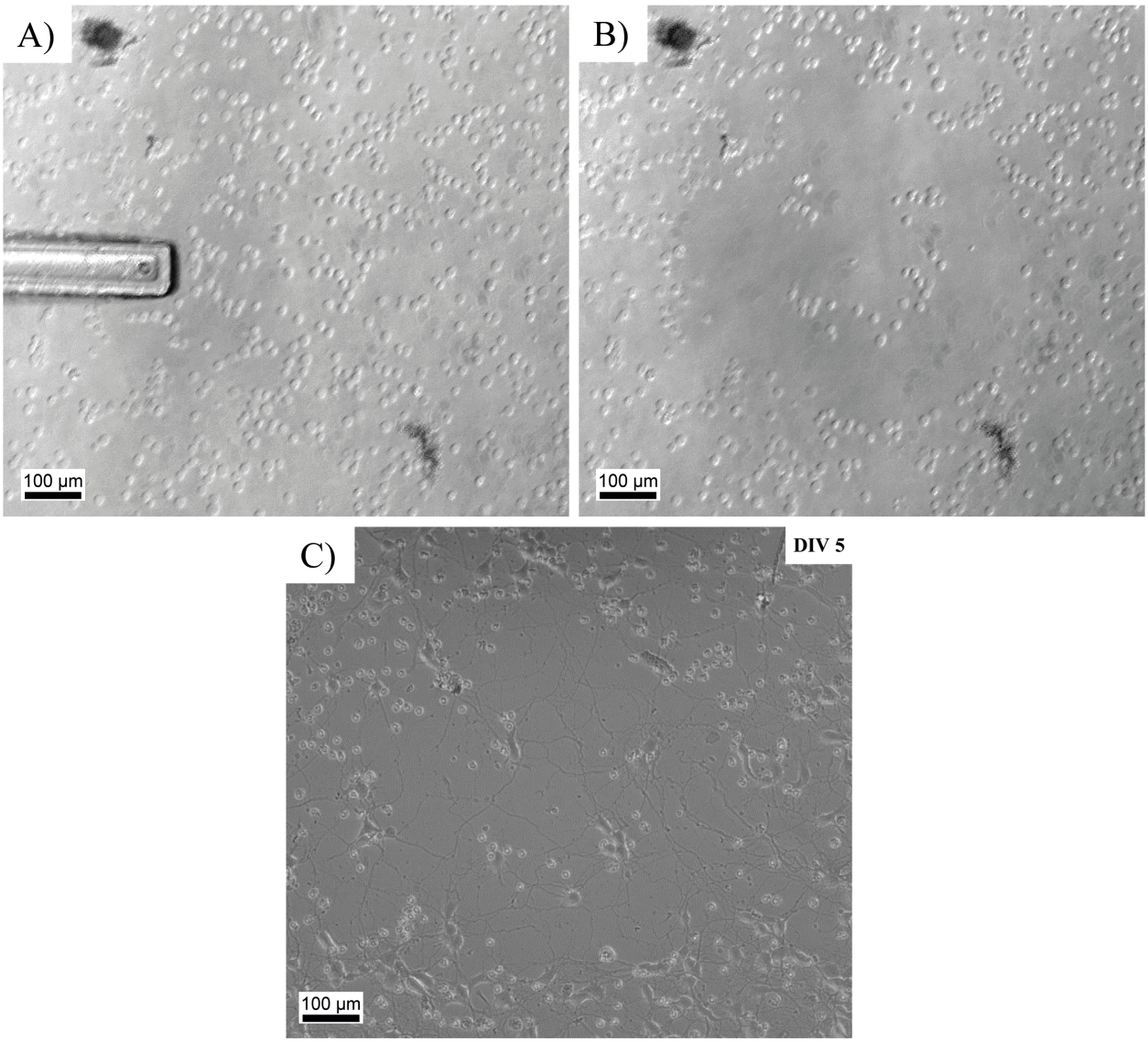

Fig. S4 Subtractive patterning of primary hippocampal neurons on a homogeneous PDL-coated adhesive surface (configuration 4). A) The culture before patterning with the cantilever used for the process. B) A negative pressure of -500 mbar was used to remove neurons in the form a pumpkin-like smiley. C) Cells of the pattern remained viable after the removal process, and despite the network development and cell migration typical for healthy cultures, the pattern was still visible after 5 DIV.

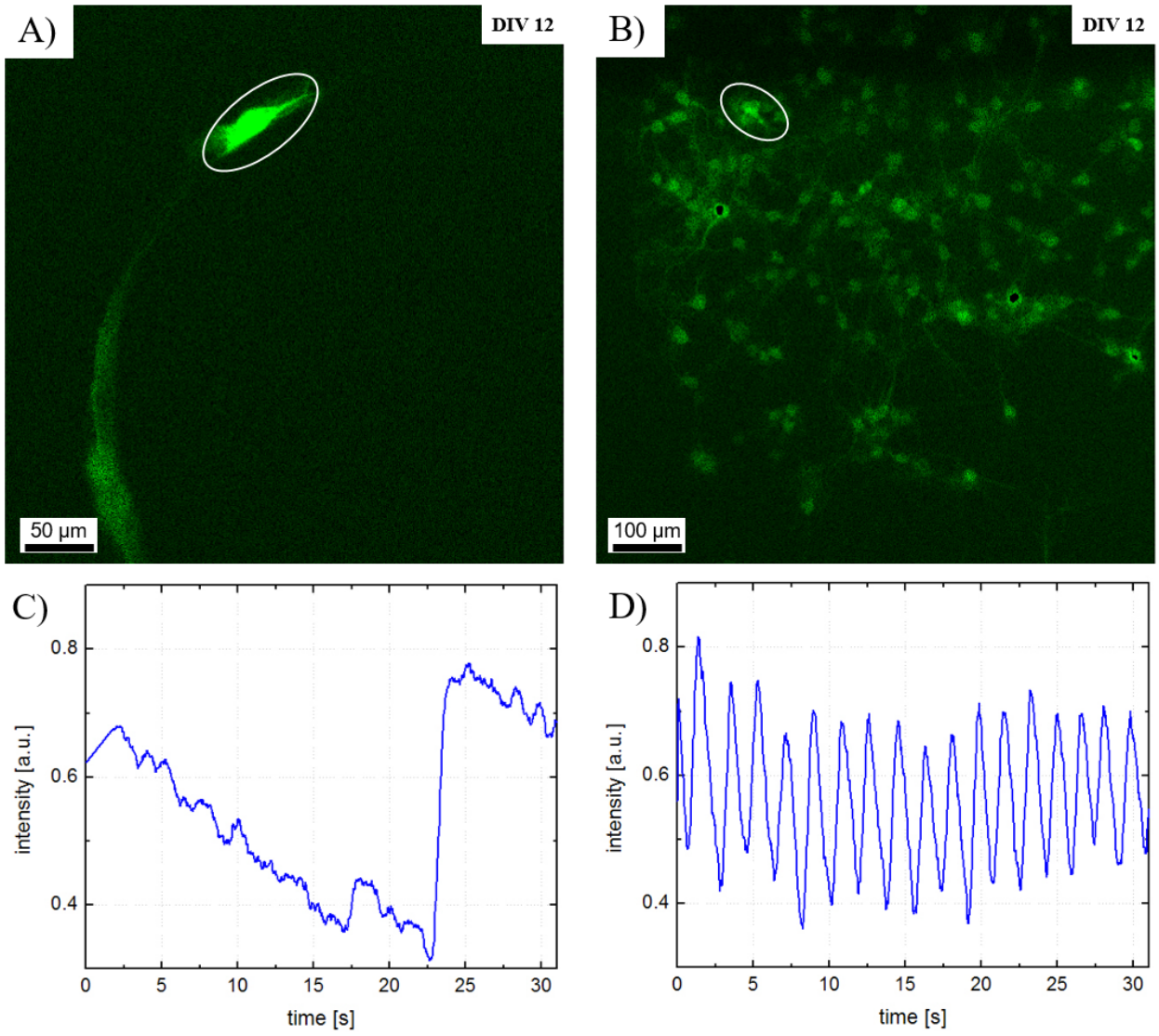

Fig. S5 Viability of the patterned cultures assessed by tracking the neuronal activity via calcium imaging. Cultures were transfected after 6 DIV to visualize the neuronal activity with the help of the calcium sensor GCaMP6. A) and B) Representative fluorescent images at 12 DIV within and close to the pattern of Fig. 5E-F, respectively. C) and D) The corresponding traces of the spontaneous activity calculated from the indicated regions of interest. See supporting movie M6 for the whole recordings, and the experimental section of the manuscript for details of the signal processing steps.

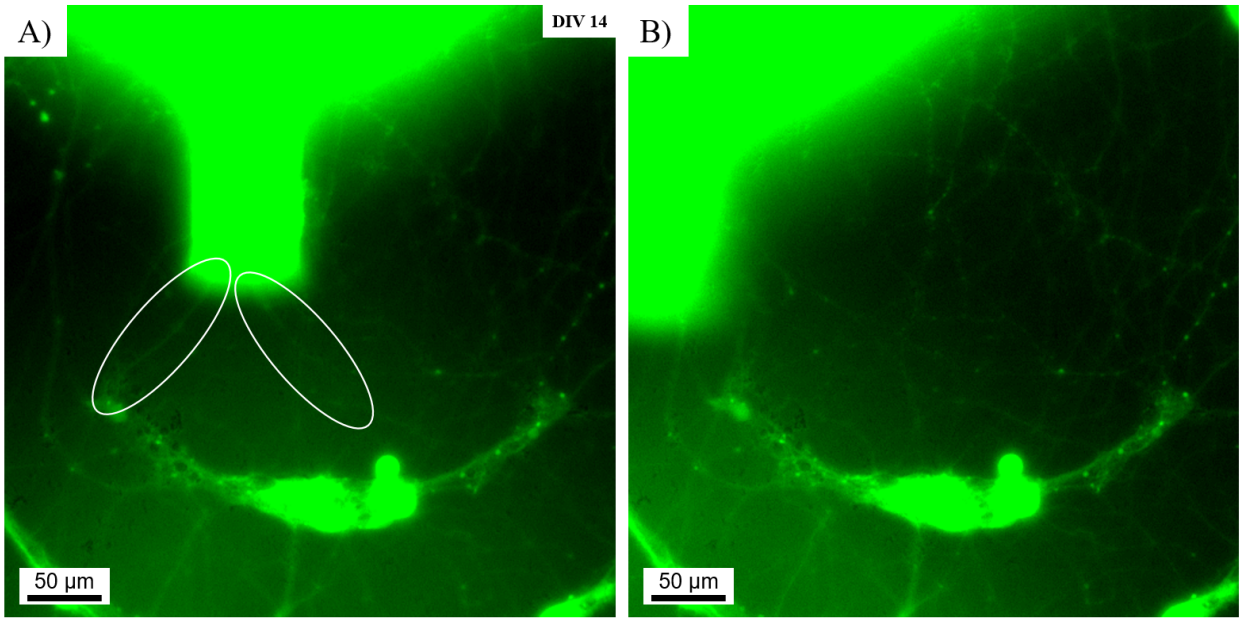

Fig. S6 Close-up view on the *in situ* modification of the smiley-like pattern of Fig. 6B at 14 DIV. A) The corresponding fluorescent image before removing the cells representing the left eye of the pattern and B) after the removal. The fluorescent signal was oversaturated in order to improve the visibility of the neuronal processes, and emphasize that those connected to the removed cells (see highlighted areas) were also disrupted during the removal process. See supporting movie M7 for the whole removal process.

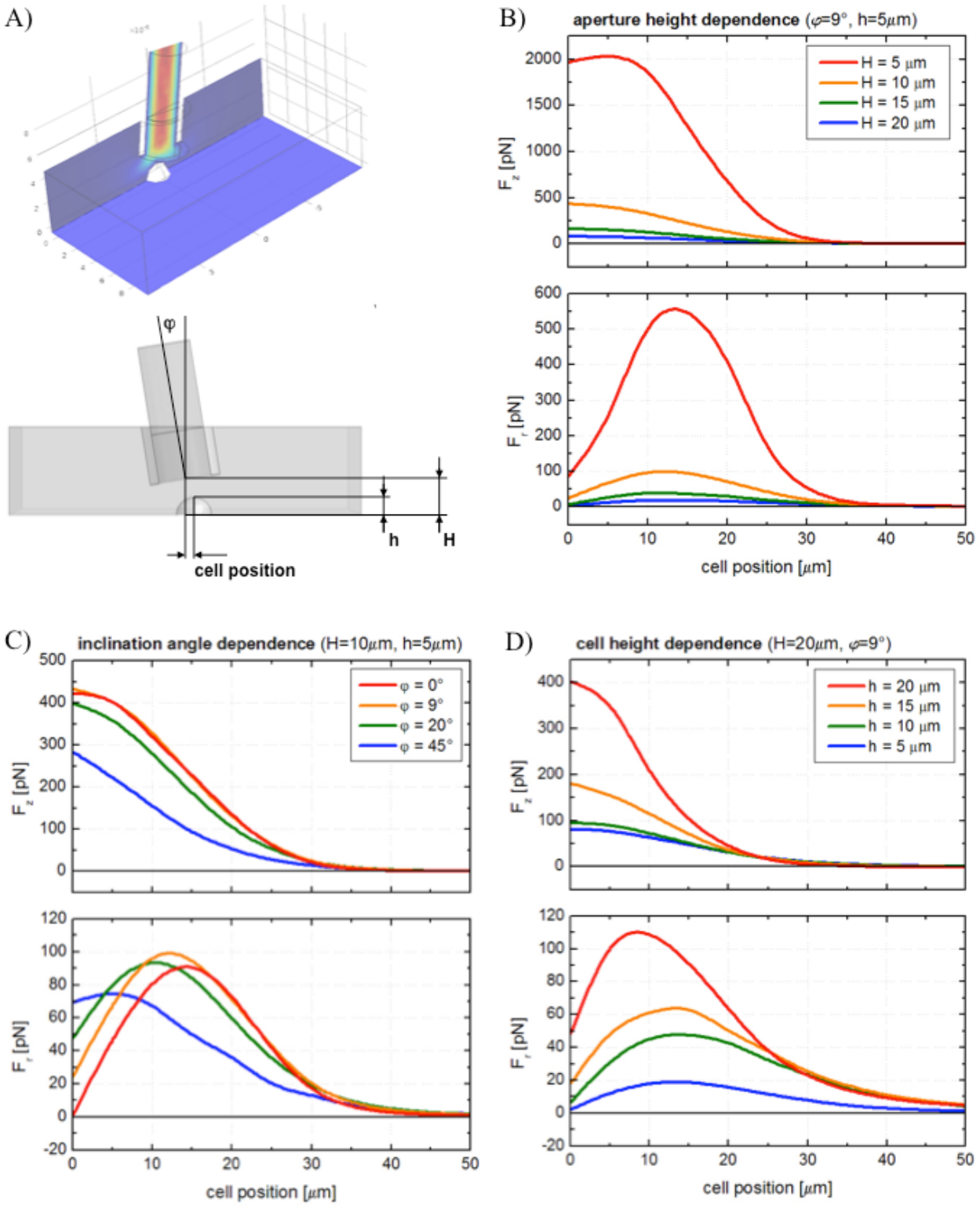

Fig. S7 A numerical simulation approximating the different force components acting on the cells during aspiration. A) The model used for the calculations. B-D) Vertical (F_z) and radial (F_r) components of the force acting on the cells as the function cell position, while changing the aperture height, aperture inclination, and cell height.

Details of the numerical simulation used for Fig. S7

A COMSOL model (COMSOL Multiphysics 5.0; COMSOL Inc., USA) has been built to approximate the different force components acting on the cells during the aspiration process of subtractive patterning. As represented in Fig. S7A, the hollow cantilever is approximated by a pipe having inner and outer diameters of 30 and 40 µm, respectively, while the cell is approximated by a spherical cap with 20 µm maximum (i.e. visible) diameter. The cell position, i.e. the horizontal distance between the centers of the cell and the aperture, as well as the aperture height (H), the aperture inclination (ϕ), and the cell height (h) have been varied to calculate the results presented in Fig. S7B-D. The model assumed laminar flow conditions and an average flow speed of 1 mm/s at the end of the pipe representing the cantilever, which value corresponds to 10 mbar applied negative pressure according to the results of Fig. S2. Due to the laminar model, the calculated forces scale with the flow speed at different values.